IOPscience iopscience.iop.org

Home Search Collections Journals About Contact us My IOPscience

Martensitic transformation B2–R in Ni–Ti–Fe: experimental determination of the Landau potential and quantum saturation of the order parameter

This article has been downloaded from IOPscience. Please scroll down to see the full text article.

2008 J. Phys.: Condens. Matter 20 275216

(http://iopscience.iop.org/0953-8984/20/27/275216)

View the table of contents for this issue, or go to the journal homepage for more

Download details:
IP Address: 129.252.86.83
The article was downloaded on 29/05/2010 at 13:25

Please note that terms and conditions apply.

J. Phys.: Condens. Matter **20** (2008) 275216 (7pp) doi:10.1088/0953-8984/20/27/275216

Martensitic transformation B2–R in Ni–Ti–Fe: experimental determination of the Landau potential and quantum saturation of the order parameter

Ekhard K H Salje[1], Huali Zhang[1], Antoni Planes[2] and Xavier Moya[2]

[1] Department of Earth Sciences, University of Cambridge, Downing Street, Cambridge CB2 3EQ, UK
[2] Departament d'Estructura i Constituents de la Matèria, Facultat de Física, Universitat de Barcelona, Diagonal 647, 08028 Barcelona, Spain

Received 27 March 2008, in final form 25 April 2008
Published 4 June 2008
Online at stacks.iop.org/JPhysCM/20/275216

Abstract
The Landau potential of the martensitic phase transformation in $Ni_{46.8}Ti_{50}Fe_{3.2}$ was determined using high resolution x-ray diffraction to measure the spontaneous strain and calorimetric measurements to determine the excess specific heat of the R phase. The spontaneous strain is proportional to the square of the order parameter which is tested by the relation of the excess entropy and the order parameter. The parameters of the Landau free energy were determined by fitting the temperature evolution of the order parameter and using the scaling between the excess entropy and the order parameter. The double well potential at absolute zero temperature was calculated and the interface energy and domain wall thickness were estimated.

(Some figures in this article are in colour only in the electronic version)

1. Introduction

NiTi alloys are among the most promising materials for shape memory applications. A large body of work has been dedicated to investigating the phase diagram and the effect of microstructures on the martensitic phase transitions [1–12]. Three phases are relevant for this paper: the cubic B2 phase ($Pm\bar{3}m$) as the austenite phase, the trigonal R phase ($P\bar{3}$) as an intermediate phase and the low temperature monoclinic B19′ phase ($P2_1/m$) [3–7, 13–16]. The martensitic R phase occurs also in relation to stress fields surrounding precipitates [17] and dislocations [11]. The R phase can be stabilized in ternary alloys including Fe, Al, or Co in addition to Ni/Ti at a roughly 50/50 mixture [7]. The observation that addition of Fe decouples transitions to R and B19′ martensites [18] was confirmed later [16, 19]. The difficulty for the investigation of the R phase is its relative instability with respect to doping, stress fields and, possibly, surface effects. In this paper we report an experimental study of a sample with the composition $Ni_{46.8}Ti_{50}Fe_{3.2}$ at temperatures between 290 and 10 K.

This investigation forms part of a wider investigation of martensitic phase transformations where we wish to clarify the thermodynamic driving force of the transformation under equilibrium conditions. The hypothesis is that the transitions can be described by Landau-type potentials while it is an open question whether additional terms are needed to reproduce the experimental observations of, say, the temperature evolution of the excess entropy or the spontaneous strain of the transformation. This approach has also consequences for the determination of the 'mechanical' potentials (namely the excess enthalpy at $T = 0$ K) which are widely used for the calculation of equilibrium textures [20–22]. Such potentials would be smooth double well potentials in the case of Landau potentials but may contain singularities otherwise.

Our investigations are also directed towards a better understanding of the energy scales involved in the phase transformation and the evolving microstructures. While a large body of experimental and theoretical work exists for ferroelastic phase transformations in ceramics [23–34] equivalent studies are rare in alloys. The reason for the scarcity

 © 2008 IOP Publishing Ltd Printed in the UK

of such data is the fact that alloys often show strongly stepwise transformations where the experimental determination of the temperature evolution of the order parameter is limited to very small intervals as it nears its value at 0 K. In addition, it has not been possible to determine the interfacial energies because the thickness of twin boundaries is too small for even the best studies in high resolution transmission electron microscopes (while oxides display thick walls of several nm width [35, 36]). Non-metallic ferroelastic materials often show phase transformations of second order or weakly first order. This makes the observation of the temperature evolution of the order parameter, e.g. via strain measurements, over a large temperature interval relatively easy. Nevertheless, as we have shown recently for the case of Ni–Al martensites [37, 38], high resolution strain measurements combined with calorimetric measurements lead to a good determination of thermodynamic potentials which, in the case of Ni–Al, do indeed follow Landau-type behavior within experimental accuracy.

It is the purpose of this paper to test whether the phase transition of Ni–Ti is correctly described in terms of Landau potentials [39, 40] as is accepted in ferroelastic non-metallic materials [26, 27, 41] and in metallic martensites such as Ni–Al [37, 38]. The first significant step towards this goal was undertaken by Khalil-Allafi *et al* [3] who determined the first Landau potentials in NiTi over a limited temperature interval of 60 K. At low temperatures the appearance of the B19′ phase disallowed the extension of the measurements to temperatures below 230 K. Data measured at lower temperatures are needed, however, to determine the quantum saturation of the order parameter [26, 33, 34, 42, 43] and the extrapolated value at absolute zero temperature. We overcame this problem by using a sample of TiNi (50/46.8) which was doped with 3.2 mol% Fe. This doping suppressed the low temperature phase so that the B2–R transition could be observed over a very large temperature interval of 260 K [16, 18, 44].

In this study, we performed high resolution x-ray measurements of spontaneous strain and calorimetric measurements on a Ni–Ti–Fe sample. We will argue in this paper that the results are in good agreement with predictions of Landau-type theories provided that the quantum saturation of the order parameter is expressed explicitly in the potentials. The resulting excess enthalpy at $T = 0$ K is a smooth double well potential with a barrier energy of 468 J mol^{-1}.

2. Experiments

A polycrystalline sample with a nominal composition of $Ni_{46.8}Ti_{50}Fe_{3.2}$ was prepared by melting high purity materials. It was then annealed at 1170 K for 600 s in controlled Ar atmosphere and then quenched in water at room temperature. The composition was confirmed by atomic absorption analysis.

X-ray diffraction (XRD) experiments were conducted using monochromatic Cu Kβ radiation and a position sensitive detector with an angular range 2θ of 120°. The distance between two channels is equivalent to a resolution of the 2θ measurement of $\Delta(2\theta) = 0.018°$; the instrumental linewidth of the diffraction signal is $\delta(2\theta) = 0.08°$. This value is mainly determined by the divergence of the incoming x-ray beam. In this experimental arrangement, the sample holder was tilted around an axis perpendicular to the x-ray beam, making it possible to record intensity-2θ spectra at different rocking angles ω [45]. The angular resolution of the rocking movement is 0.001°. For regular measurements, the sample holder continually rocks over an angular range where the relevant x-ray peaks are located. The x-ray spectra were recorded on a cooling process from 290 to 10 K at a step of 5 K. The width of the rocking signal of the (110) diffraction signal in the austenite phase is 0.3° (full width at half maximum).

The specific heat was measured by means of a modulated differential scanning calorimeter (MDSC) under static conditions (each data point was obtained by keeping the temperature constant) [46]. For the determination of the latent heat a highly sensitive differential scanning calorimeter (DSC) was used.

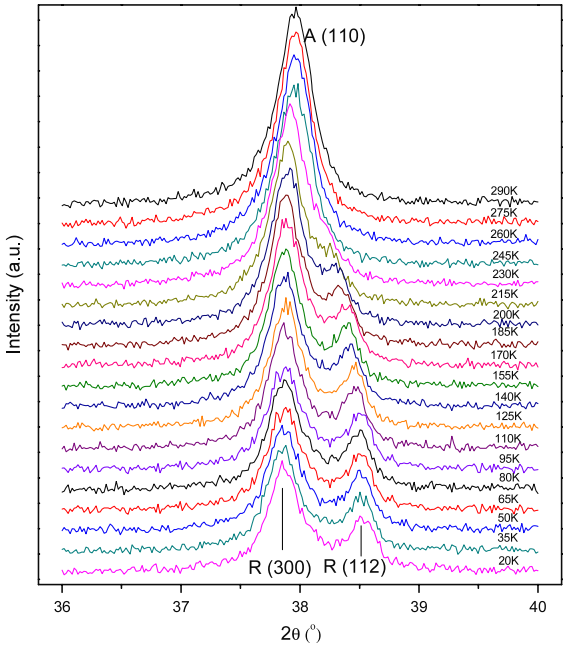

Figure 1. Temperature evolution of the austenite (110) peak on cooling into the (300)/(112) doublet of the R phase. For clarity the intensities of the spectra were displaced along the ordinate.

3. Results

Figure 1 shows (110) diffraction maximum of austenite evolving into the (300)/(112) doublet of the R phase. The splitting of the doublet increases with decreasing temperature. The peak positions were obtained by careful curve fitting with Lorentz functions. Figure 2 shows the temperature dependence of the lattice spacings of the R phase of the (112) and (300) diffraction signals and the equivalent spacing from the austenitic (110) peak. The spontaneous strain (self-strain) of the phase transformation is related to the rhombohedricity of the R phase which can be calculated from the splitting of the (300)/(112) doublet [3], $\varepsilon = 2(d_{300} - d_{112})/(d_{300} + d_{112})$, as shown in figure 3. The error in the determination of the temperature evolution of the spontaneous strain is estimated to be below 2%.

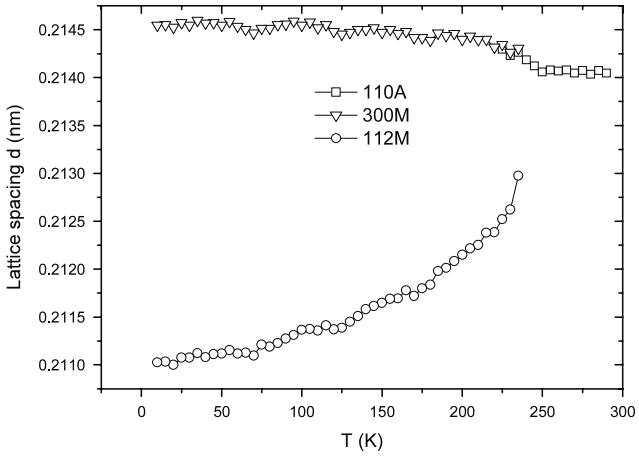

Figure 2. Temperature evolution of the lattice spacing $d_{(110)}$ in austenite and its martensitic equivalents $d_{(112)}$ and $d_{(300)}$.

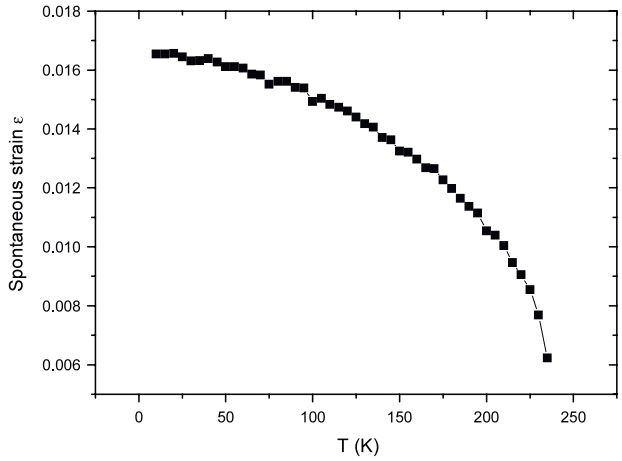

Figure 3. Temperature evolution of the spontaneous strain of the R phase with $\varepsilon = 2(d_{300} - d_{112})/(d_{300} + d_{112})$.

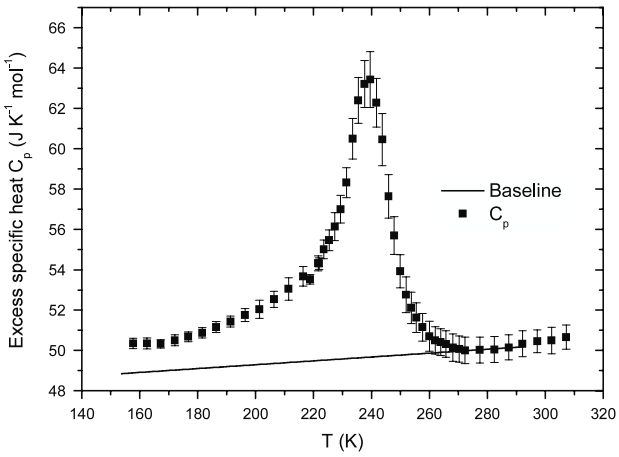

Figure 4. Temperature dependence of the specific heat.

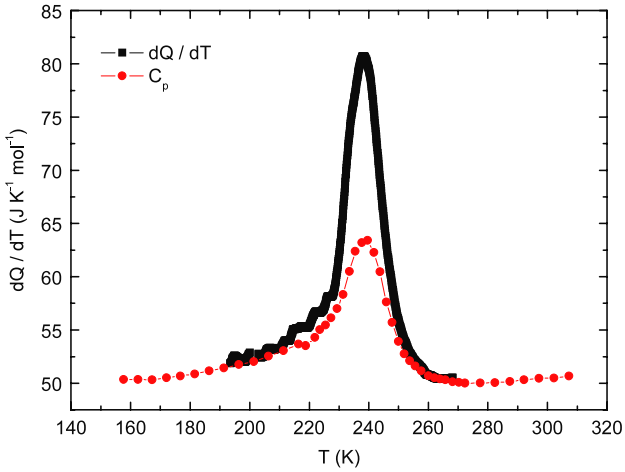

Figure 5. DSC thermogram under cooling and the temperature dependence of the specific heat.

Figure 4 shows the temperature dependence of the specific heat. The error bars for the specific heat are also shown in the figure and are below 2%. As base line we constructed a linear extrapolation of the specific heat data at high temperatures. Figure 5 shows the DSC thermogram under cooling and the temperature dependence of the specific heat. The latent heat only occurs at the transition temperature region while outside this region the DSC curve overlaps with the specific heat contribution. The area limited by the two curves gives the latent heat associated with the transition. The excess entropy was determined by integrating the excess specific heat $S(T) = -\int_{T}^{T_{\text{trans}}} \frac{\Delta C_p}{T}\,\mathrm{d}T$. The latent heat contribution obtained from figure 5 was included at the transition temperature.

4. Application of Landau potential

The classic Landau potential for first order phase transition in the displacive limit for the relevant symmetry constraints is a 2-4-6 model

$$G(Q) = \tfrac{1}{2}A(T - T_{\text{c}})Q^2 + \tfrac{1}{4}BQ^4 + \tfrac{1}{6}CQ^6 + \tfrac{1}{2}g(\nabla Q)^2, \quad (1)$$

where Q is the order parameter; T is the temperature; T_{c} is the Curie temperature and A, B, and C are energy scaling parameters related to local potentials [24]; g is the Ginzburg parameter describing the energy involved in the formation of heterogeneous structures. The expression in equation (1) is limited to sixth order potentials in order to keep the number of free parameters small; higher order terms were discussed by Barsch and Krumhansl [47]. Although this model can predict the transition behavior at high temperature very well, it is known that this model cannot simply be extrapolated to low temperatures. The underlying difficulty relates to the third law of thermodynamics, which implies that the absolute zero temperature cannot be attained. A direct consequence of this is that $\mathrm{d}Q/\mathrm{d}T \to 0$ as $T \to 0$. The saturation behavior is driven by thermodynamic effects, and not because the order parameter has reached some maximum value, which can never be exceeded. To take account of these effects in displacive phase transitions under the most commonly encountered circumstances [23, 24], it is sufficient to modify the quadratic term in equation (1). The resulting quantum version of Landau theory of first order phase transitions under the relevant symmetry constraints is expressed by a

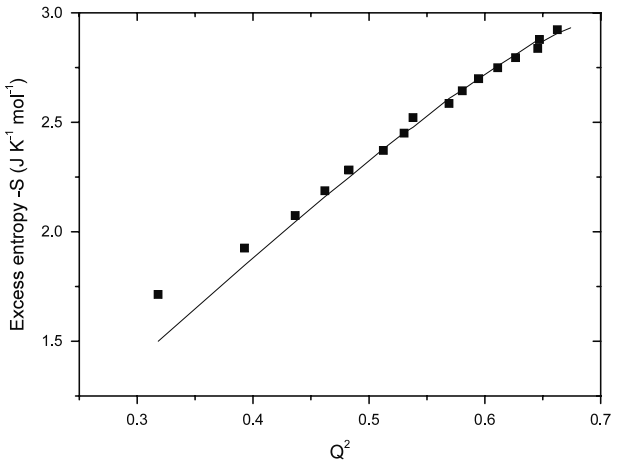

Figure 6. Excess entropy versus Q^2. The fit line shows the relation $S(Q) = -\frac{1}{2}A\Theta_s^2(\coth^2\frac{\Theta_s}{T} - 1)Q^2/T^2$ with $A = 10.1$ J K^{-1} mol^{-1}, $\Theta_s = 102.7$ K.

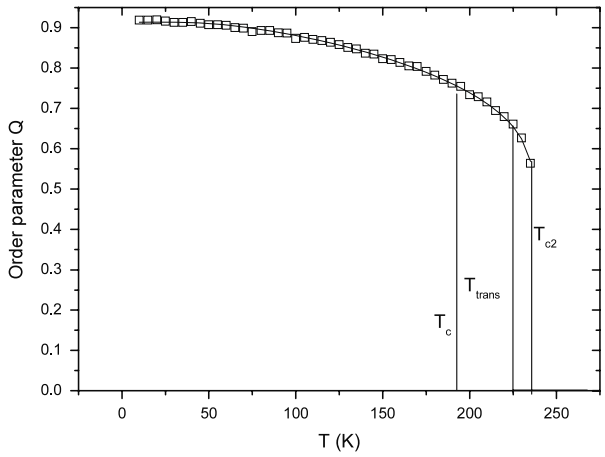

Figure 7. Temperature dependence of order parameter and the fit line with equation (3) with $A = 10.1$ J K^{-1} mol^{-1}, $B = -2816.9$ J mol^{-1}, $C = 4937.9$ J mol^{-1}, $T_c = 192.8$ K, $\Theta_s = 102.7$ K, $T_{trans} = 225.1$ K. $T_{c2} = 235.7$ K is the highest temperature with a local free energy minimum for the martensitic phase.

macroscopic Gibbs free energy [23, 24]

$$G(Q) = \tfrac{1}{2}A\Theta_s\left(\coth\frac{\Theta_s}{T} - \coth\frac{\Theta_s}{T_c}\right)Q^2 + \tfrac{1}{4}BQ^4 + \tfrac{1}{6}CQ^6 + \tfrac{1}{2}g(\nabla Q)^2, \quad (2)$$

where Θ_s is the quantum mechanical saturation temperature which characterizes the temperature of the crossover between classical and quantum mechanical behavior. This quantum version is valid for both high and low temperatures. The equilibrium of the order parameter is given by the minimum of the free energy. The equilibrium condition $\mathrm{d}G(T)/\mathrm{d}Q = 0$ applied to equation (2) leads to the temperature dependence of the square of the order parameter:

$$Q^2 = \frac{-B + \sqrt{B^2 + 4AC\Theta_s(\coth\frac{\Theta_s}{T_c} - \coth\frac{\Theta_s}{T})}}{2C}. \quad (3)$$

The B2–R phase transition is of the paraelastic to improper ferroelastic type, thus the spontaneous strain follows the square of the primary order parameter Q. A test for the validity of this approach follows from the scaling of the excess entropy which is related to the order parameter via $S(Q) = -\mathrm{d}G(Q)/\mathrm{d}T$. At $T \gg \Theta_s$ this leads to a simple scaling $S(Q) = -\frac{1}{2}AQ^2$. Including the quantum saturation the approximation of the scaling derived from equation (2) becomes $S(Q) = -\frac{1}{2}A\Theta_s^2(\coth^2\frac{\Theta_s}{T} - 1)Q^2/T^2$.

For convenience it is customary to normalize the order parameter to unity at absolute zero temperature for vanishing quantum saturation (details mentioned later). Figure 6 shows the relation between excess entropy S and the square of order parameter Q^2. The fit line shows the $S(Q) = -\mathrm{d}G(Q)/\mathrm{d}T$ relation with saturation temperature $\Theta_s = 102.7$ K. The agreement between the theoretical curve and the data points is excellent; the larger systematic deviations for the two lowest data points for the lowest entropy values are due to the influence of the latent heat on the specific heat data in the transition region.

The temperature evolution of the order parameter was determined from the spontaneous strain data with $Q = (\varepsilon/\varepsilon_0)^{1/2}$ and Landau potential parameters were obtained by fitting the order parameter with equation (3), as shown in figure 7. ε_0 is the spontaneous strain at absolute zero temperature without quantum saturation and the value was chosen to make sure the order parameter has value 1 at absolute zero temperature when mathematically switching the quantum saturation off (i.e. setting Θ_s to zero). The coexistence intervals obtained from the potential parameters are also shown in figure 7. The stability limit of the martensite agrees well with the experimental data. Figure 8 shows the thermodynamic potentials (as molar excess free energy) versus order parameter at different temperatures.

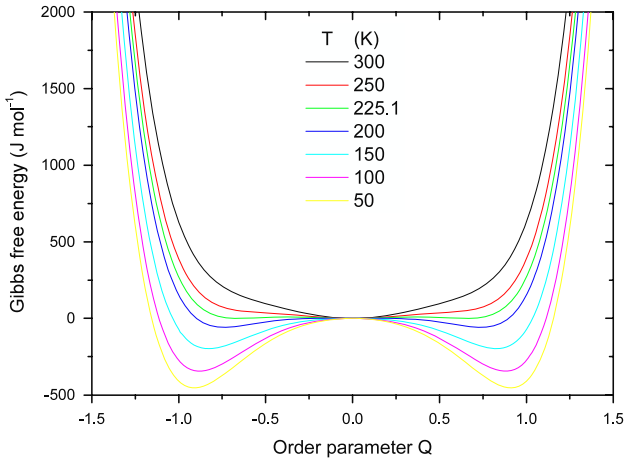

Figure 8. Gibbs free energy versus order parameter at different temperatures.

Note that the saturation temperatures which were obtained independently from the scaling of the excess entropy with the order parameter and by fitting the order parameter to equation (3) agree very well. The good agreement between the fitted and measured temperature evolution of the order parameter clearly indicates the validity of the approach and the self-consistency of the thermodynamic modeling of martensitic

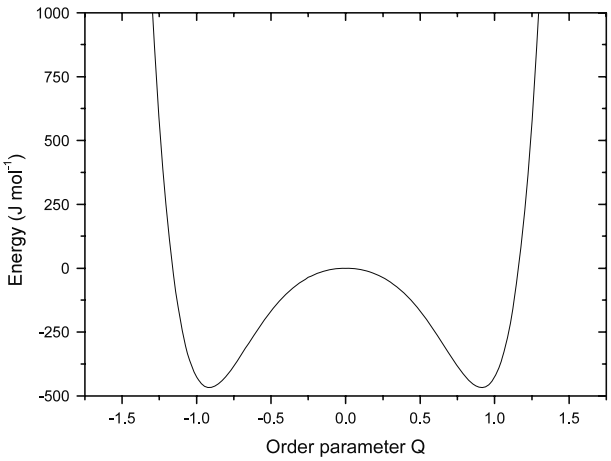

Figure 9. Double well 'mechanical' potential at 0 K calculated from the obtained Landau potential.

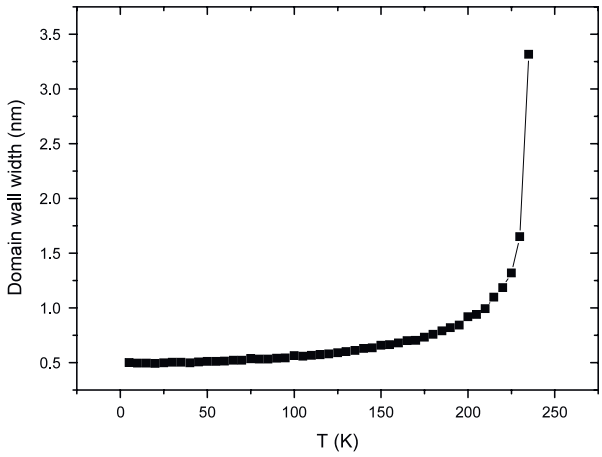

Figure 10. Estimated upper bound for the temperature dependence of the domain wall width.

transitions in terms of Landau potentials. Typically, a phase transition behaves classically for $T > \frac{3}{2}\Theta_s$, the effect of the quantum saturation of the order parameter becomes noticeable only at temperatures below $2\Theta_s$ near 200 K. This covers most of the experimentally accessible temperature range in the R phase so that the saturation temperature is quite well constrained.

The Debye temperatures of $Ti_{50}Ni_{48}Fe_2$ and $Ti_{50}Ni_{47}Fe_3$ obtained by specific heat are around 350 and 275 K [44]. For the simplest case, a simple acoustic soft mode coupled to all the hard modes, we expect the Θ_s to be related to the Einstein temperature (or the Debye temperature, we do not distinguish between either in this approximation) via $\Theta_s = \frac{1}{2}\Theta_E$. The value of our result is $\Theta_s = 102.7$ K which would correspond to $\Theta_E = 205$ K. The value is slightly lower than the reported value, which shows that the coupling between the soft mode and other dynamical excitations in NiTiFe is relatively strong [33, 34]. The general observation in phase transitions such as in quartz is that the saturation value lies between the temperature equivalent of the soft mode and half the Debye temperature in the case that the order parameter couples with the full heat bath [48]. The experimental observations are in full agreement with a displacive nature of the phase transformation.

The double well potential (i.e. the enthalpy H at 0 K) calculated from the obtained Landau potential is shown in figure 9. The excess enthalpy at zero K is -468 J mol^{-1} (or -4.9 meV per formula unit). This value represents the height of the local maximum in the 'mechanical' double well potential.

As the observations show that the thickness of domain walls in martensites is only a few lattice parameters wide, we set $w = 0.5$ nm at 0 K as an upper limit. The width of a twin domain wall is given by the length scale

$$w^2 = \frac{2g}{BQ^2(1 + 2Q^2C/B)} \tag{4}$$

for a first order phase transition [23], so we obtained the Ginzburg parameter $g = 5.67 \times 10^{-16}$ J m^2 mol^{-1}. This value is smaller than equivalent Ginzburg parameters in anorthoclase, 4×10^{-15} J m^2 mol^{-1} (calibrated by the data in [49, 50]) and in $YBa_2Cu_3O_7$, 5×10^{-15} J m^2 mol^{-1} [51] and larger than in Ni–Al, 6×10^{-17} J m^2 mol^{-1} [37].

The interface energy at 0 K is then estimated [23] to be $E_0 = w\Delta H = 14 \times 10^{-3}$ J m^{-2}. The lower estimate of the wall energy is 2.8×10^{-3} J m^{-2} if the wall thickness is taken to be 0.1 nm. This interface energy is similar to the values found in $SrTiO_3$, namely 4×10^{-4} J m^{-2} [52] or, in a different approximation 1.3×10^{-3} J m^{-2} [45], in $In_{0.79}Tl_{0.21}$, 1.1×10^{-3} J m^{-2} [53], in $BaTiO_3$ for the 90° wall 4×10^{-3} J m^{-2} and the 180° wall 10×10^{-3} J m^{-2} [54], and in CuAlNi, 70×10^{-3} J m^{-2} [55].

In figure 10 the temperature dependence of wall thickness was calculated by equation (4) using the temperature evolution of the order parameter in figure 7, and the Landau potential parameters with the value of g obtained above. The wall thickness increases with temperature although there is no criticality (i.e. infinite value) at the transition temperature, as would be expected in the approximation for a second order phase transition [45].

We can now compare this potential with those of other materials in table 1. The values of A and C for Ni–Ti–Fe are similar to those in Ni–Ti while the B-parameter is more negative. These alloys have been thoroughly analyzed in terms of their respective Landau potentials. It is useful, therefore, to analyze the stepwise character of the phase transformation in Ni–Ti–Fe within the same framework as the other alloys. The step in the order parameter at T_{trans} disappears when B approaches zero. This condition $B = 0$ is called a tricritical point. The measure for the distance from the tricritical point is the parameter $B^2/4AC$ which is then compared with the temperature $\Theta_s \coth \frac{\Theta_s}{T_c}$ (or T_c for the classical version) of the Landau potential. If we normalize this closeness parameter by $\Theta_s \coth \frac{\Theta_s}{T_c}$ we find $B^2/4AC\Theta_s \coth \frac{\Theta_s}{T_c} = 0.19$ in Ni–Ti–Fe. This value is between the same parameter for Ni–Ti, 0.05, and Ni–Al, 0.38. This comparison shows that Ni–Ti–Fe has a more strongly stepwise character than Ni–Ti but less than Ni–Al and Cu–Zn–Al [37].

Table 1. Renormalized Landau potential parameters of some martensitic phase transitions.

Compound	A (J K^{-1} mol^{-1})	B (J mol^{-1})	C (J mol^{-1})	T_c (K)	Θ_s (K)
Ni–Ti–Fe	10.1	−2816.9	4937.9	192.8	102.7
Ni–Al [37, 38]	5.6	−3493	4901	86	257
Ni–Ti[a]	10.9	−1758.8	4825.2	282	

[a] Calculated from data in [3] with normalization condition $Q(0\ \mathrm{K}) = 1$.

5. Conclusion

The order parameter of the martensitic phase transition of $Ni_{46.8}Ti_{50}Fe_{3.2}$ was determined from the experimentally determined temperature evolution of the lattice deformation of the phase transition. Scaling the resulting entropy with the square of the order parameter and fitting the temperature dependence of the order parameter results in a Gibbs free energy of the transition

$$G(Q) = \frac{1}{2}A\Theta_s\left(\coth\frac{\Theta_s}{T} - \coth\frac{\Theta_s}{T_c}\right)Q^2 + \frac{1}{4}BQ^4 + \frac{1}{6}CQ^6$$

with $A = 10.1$ J K^{-1} mol^{-1}, $B = -2816.9$ J mol^{-1}, $C = 4937.9$ J mol^{-1}, $T_c = 192.8$ K, $\Theta_s = 102.7$ K, $T_{trans} = 225.1$ K and a step of the order parameter at the transition point of 0.654.

This is the first full determination of a Landau potential in a martensite including the quantum saturation of the order parameter which extends over a large temperature interval of over 200 K. The good agreement between the predicted and measured temperature evolution of the order parameter clearly indicates the validity of the approach and the self-consistency of the thermodynamic modeling of martensitic transitions in terms of Landau potentials.

Acknowledgment

Support from Marie-Curie RTN Multimat (contract No. MRTN-CT-2004-505226) is acknowledged.

References

[1] Massalski T B 1990 *Binary Alloy Phase Diagrams* 2nd edn (Metals Park, OH: American Society for Metals)
[2] Schmahl W W, Khalil-Allafi J, Hasse B, Wagner M, Heckmann A and Somsen C 2004 *Mater. Sci. Eng.* A **378** 81
[3] Khalil-Allafi J, Schmahl W W and Toebbens D M 2006 *Acta Mater.* **54** 3171
[4] Sitepu H, Schmahl W W, Reinecke T, Khalil-Allafi J and Eggeler G 2003 *J. Physique Coll.* IV **112** 677
[5] Hara T, Ohba T, Okunishi E and Otsuka K 1997 *Mater. Trans. JIM* **38** 11
[6] Hara T, Ohba T and Otsuka K 1995 *J. Physique Coll.* IV **5** 641
[7] Ren X, Minura N, Zhang J, Otsuka K, Tanaka K, Koiwa M, Suzuki T, Chumlaykov Y I and Asai M 2001 *Mater. Sci. Eng.* A **312** 196
[8] Xie C Y, Zhao L C and Lei T C 1990 *Scr. Metall. Mater.* **24** 1753
[9] Chen Q, Wu X F and Ko T 1993 *Scr. Metall. Mater.* **29** 49
[10] Fukuda T, Saburi T, Doi K and Nenno S 1992 *Mater. Trans. JIM* **33** 271
[11] Stroz D, Bojarski Z, Ilczuk J, Lekston Z and Morawiec H 1991 *J. Mater. Sci.* **26** 1741
[12] Morawiec H, Stroz D and Chrobak D 1995 *J. Physique Coll.* IV **5** 205
[13] Goryczka T and Morawiec H 2003 *J. Physique Coll.* IV **112** 693
[14] Schryvers D and Potapov P L 2003 *J. Physique Coll.* IV **112** 751
See also Schryvers D and Potapov P L 2002 *Mater. Trans. JIM* **43** 774
[15] Goryczka T and Morawiec H 2004 *J Alloys Compounds* **367** 137
[16] Salamon M B, Meichle M E and Wayman C M 1985 *Phys. Rev.* B **31** 7306
[17] Bataillard L, Bidaux J E and Gotthardt R 1998 *Phil. Mag.* A **78** 327
[18] Matsumoto M and Honma T 1976 *Trans. Japan Inst. Met.* **17** (Suppl.) 199
[19] Satija S K, Shapiro S M, Salamon M B and Wayman C M 1984 *Phys. Rev.* B **29** 6031
[20] Wang L X and Melnik R V N 2007 *Appl. Math. Modelling* **31** 2008
[21] Ball J M 2004 *Mater. Sci. Eng.* A **378** 61
[22] Ball J M and James R D 1987 *Arch. Ration. Mech. Anal.* **100** 13
[23] Salje E K H 1993 *Phase Transitions in Ferroelastic and Co-elastic Crystals* (Cambridge: Cambridge University Press)
[24] Salje E K H, Wruck B and Thomas H 1991 *Z. Phys.* B **82** 399
[25] Harrison R J, Redfern S A T and Salje E K H 2004 *Phys. Rev.* B **69** 144101
[26] Salje E K H, Gallardo M C, Jiménez J, Romero F J and del Cerro J 1998 *J. Phys.: Condens. Matter* **10** 5535
[27] Carpenter M A, Salje E K H and Graeme-Barber A 1998 *Am. Mineral.* **83** 2
[28] Gibaud A, Shapiro S M and Nouet J 1991 *Phys. Rev.* B **44** 2437
[29] Zhang M, Salje E K H, Bismayer U, Unruh H G, Wruck B and Schmidt C 1995 *Phys. Chem. Mineral.* **22** 41
[30] Salje E, Schmidt C and Bismayer U 1993 *Phys. Chem. Mineral.* **19** 502
[31] Salje E, Devarajan V and Bismayer U 1983 *J. Phys. C: Solid State Phys.* **16** 5233
[32] Speer D and Salje E 1986 *Phys. Chem. Miner.* **13** 17
[33] Pérez-Mato J M and Salje E K H 2000 *J. Phys.: Condens. Matter* **12** L29
[34] Pérez-Mato J M and Salje E K H 2001 *Phil. Mag. Lett.* **81** 885
[35] Wruck B, Salje E K H, Zhang M, Abraham A R and Bismaye U 1994 *Phase Transit.* **48** 135
[36] Tsai F, Khiznichenko V and Cowley J M 1992 *Ultramicroscopy* **45** 55
[37] Salje E K H, Zhang H, Schryvers D and Bartova B 2007 *Appl. Phys. Lett.* **90** 221903
[38] Zhang H, Salje E K H, Schryvers D and Bartova B 2008 *J. Phys.: Condens. Matter* **20** 55220
[39] Barsch G R, Ohba T and Hatch D M 1999 *Mater. Sci. Eng.* A **273–275** 161
[40] Barsch G R 2000 *Mater. Sci. Forum* **327/328** 367
[41] Hayward S A, Redfern S A T and Salje E K H 2002 *J. Phys.: Condens. Matter* **14** 10131
[42] Salje E, Wruck B and Marais S 1991 *Ferroelectrics* **124** 185

[43] Hayward S A and Salje E K H 2002 *J. Phys.: Condens. Matter* **14** L599
[44] Choi M S, Fukuda T and Kakeshita T 2005 *Scr. Mater.* **53** 869
[45] Chrosch J and Salje E K H 1999 *J. Appl. Phys.* **85** 722
[46] Boller A, Jin Y and Wunderlich B 1994 *J. Therm. Anal.* **42** 307
[47] Barsch G R and Krumhansl J A 1984 *Phys. Rev. Lett.* **53** 1069
[48] Romero F J, Gallardo M C, Hayward S A, Jiménez J, del Cerro J and Salje E K H 2004 *J. Phys.: Condens. Matter* **16** 2879
[49] Hayward S A, Chrosch J, Salje E K H and Carpenter M A 1996 *Eur. J. Mineral.* **8** 1301
[50] Hayward S A and Salje E K H 1996 *Am. Mineral.* **81** 1332
[51] Chrosch J and Salje E K H 1994 *Physica* C **225** 111
[52] Cao W and Barsch G R 1990 *Phys. Rev.* B **41** 4334
[53] Barsch G R and Krumhansl J A 1988 *Metall. Trans.* A **19** 761
[54] Bulgaevskii L N 1964 *Sov. Phys.—Solid State* **5** 2329
[55] Shilo D, Mendelovich A and Novák V 2007 *Appl. Phys. Lett.* **90** 193113